

# Microstructural Evolution in Interdiffusion Zone and Its Effect on Diffusion Path

---

K. Wu, J. E. Morral and Y. Wang

Department of Materials Science and Engineering  
The Ohio State University

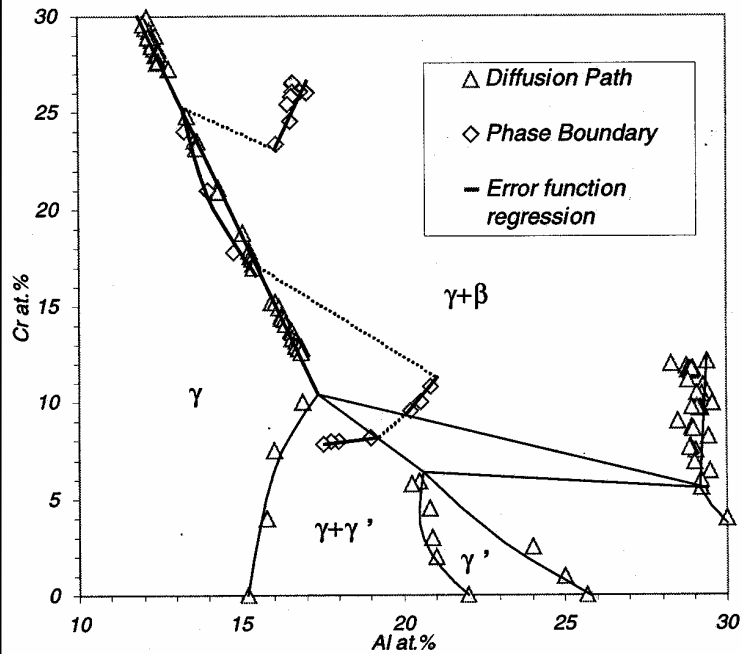
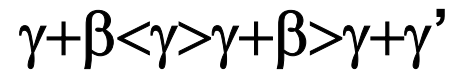


Work Supported by NSF

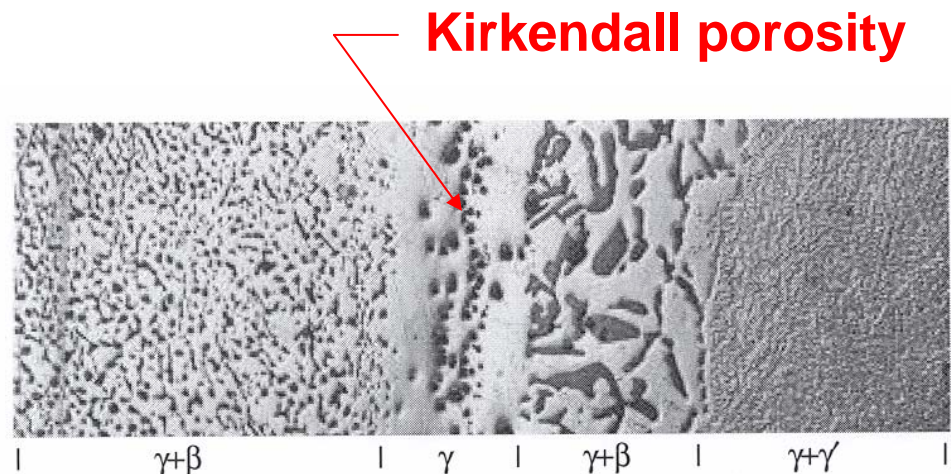
TMS05 Annual Meeting  
Feb. 13-17, 2005, San Francisco, California



# Experimental Observation of Interdiffusion Microstructure and Diffusion Path



(c) Diffusion path of diffusion couple



(d) Microstructure of diffusion couple

Xin Qiao. M.S. Thesis. University of Connecticut. 1998



# The Multicomponent Mountain

Predict Interdiffusion  
Microstructure

Five-line nodes

Interdiffusion microstructure maps

Short hand notation

Three types of boundary

Zigzag diffusion paths

Kirkendall porosity

Zero-Flux Planes

Diffusivity measurements

Square root diffusivity

Amount of Interdiffusion

Composition Vector



# The Other Side of the Multicomponent Mountain

Predict Interdiffusion  
Microstructure



High Temp. Coatings

Soldering and Brazing

Diffusion bonding

Phase Transformations

Carburizing, Nitriding

Powder Processing

# Climbing the Multicomponent Mountain with John

## Coupling interdiffusion with microstructural evolution:

- Effect of two-phase microstructure on interdiffusion and diffusion path
- Interdiffusion induced phase and microstructure instabilities
- Effect of concentration gradient on nucleation, growth and coarsening
- Effect of phase transformation on interdiffusion
- Roles of coherency/thermal stress on interdiffusion and phase transformation

## Predict Interdiffusion Microstructure

Phase Field

Five-line nodes

Interdiffusion microstructure maps

Short hand notation

Three types of boundary

Zigzag diffusion paths

Kirkendall porosity

Zero-Flux Planes

Diffusivity measurements

Square root diffusivity

Amount of Interdiffusion

Composition Vector

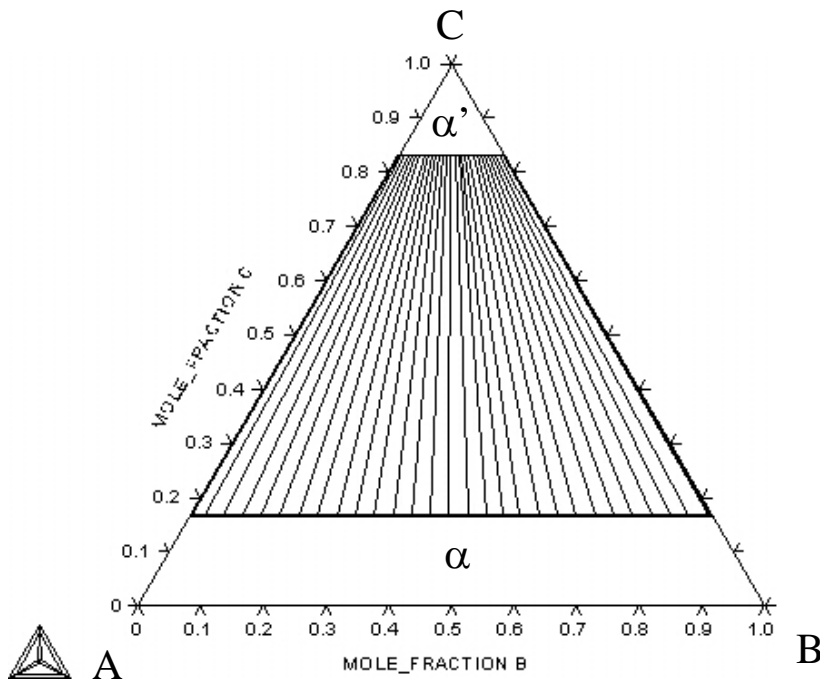
- One-dimensional diffusion in a common matrix phase
- Precipitates are treated as stationary point sources or sinks of solute
- Mutual interactions between microstructure and interdiffusion and corresponding effects on diffusion path and microstructural evolution are ignored



# Simple Model System

## Free energy model

$$G_m = RT (X_A \ln X_A + X_B \ln X_B + X_C \ln X_C) + I (X_A X_C + X_B X_C)$$



- Elements A and B form ideal solution while elements A and C or B and C form regular solutions

*Wu et. al. Acta mater. 2001;49:3401*

*Wu et. al. Acta mater, 2004; 52:1917*

# Phase Field Equations

---

$$\left. \begin{aligned} \frac{\partial X_B}{\partial t} &= \nabla \left[ M_{11} \nabla (\mu_B - \mu_A) \right] + \nabla \left[ M_{12} \nabla (\mu_C - \mu_A) \right] \\ \frac{\partial X_C}{\partial t} &= \nabla \left[ M_{21} \nabla (\mu_B - \mu_A) \right] + \nabla \left[ M_{22} \nabla (\mu_C - \mu_A) \right] \end{aligned} \right\} \text{Diffusion equations}$$

$$\left. \begin{aligned} \mu_B - \mu_A &= \mu_B^B - \mu_A^B - 2\kappa_{11} \nabla^2 X_B - 2\kappa_{12} \nabla^2 X_C \\ \mu_C - \mu_A &= \mu_C^B - \mu_A^B - 2\kappa_{21} \nabla^2 X_B - 2\kappa_{22} \nabla^2 X_C \end{aligned} \right\} \text{Gradient thermodynamics}$$

$$\left. \begin{aligned} M_{11} &= \rho X_B \left[ (1 - X_B)^2 \beta_B + X_B X_C \beta_C + X_B X_A \beta_A \right] \\ M_{12} = M_{21} &= \rho X_B X_C \left[ -(1 - X_B) \beta_B - (1 - X_C) \beta_C + X_A \beta_A \right] \\ M_{22} &= \rho X_C \left[ X_B X_C \beta_B + (1 - X_C)^2 \beta_C + X_C X_A \beta_A \right] \end{aligned} \right\} \text{Kinetics parameters}$$

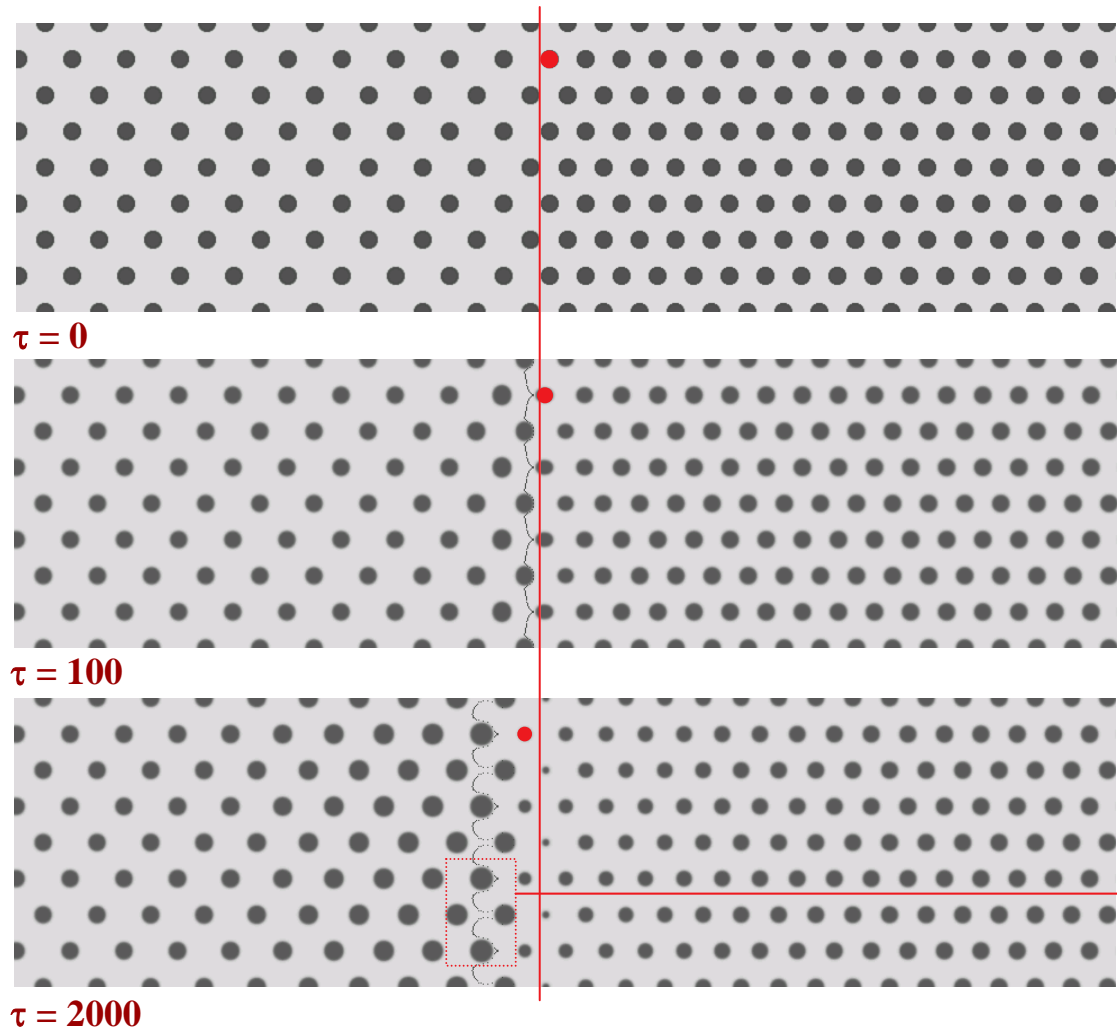
$M_{ij}$  - chemical mobilities  
 $\kappa_{ij}$  - gradient coefficients  
 $\beta_i$  - atomic mobilities  
 $\rho$  - molar density

Wu et. al. *Acta mater.* 2001;49:3401

Wu et. al. *Acta mater.* 2004; 52:1917



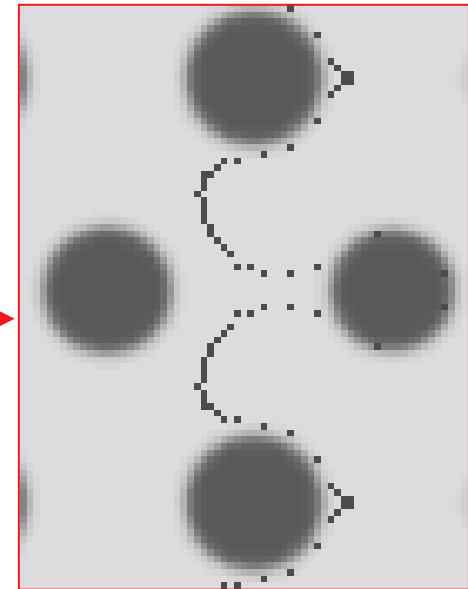
# Interaction between Microstructure and Interdiffusion – Type 0 boundary



$$\beta_B=1.0 \quad \beta_C=5.0 \quad \beta_A=10.0$$

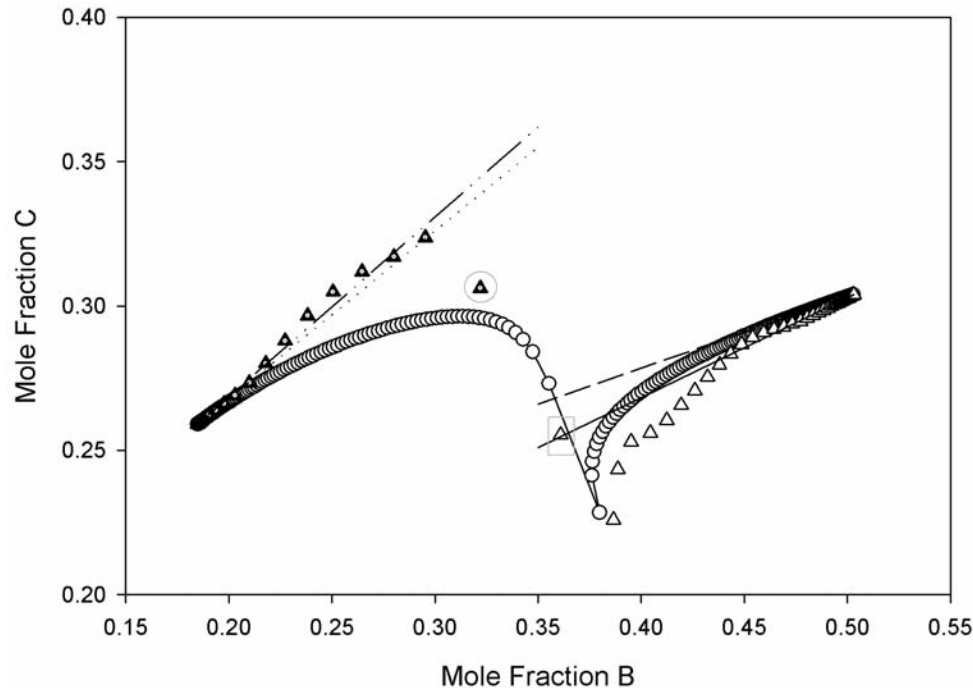
4608x64 size simulation, 1024x256 size output

- Ppt and Type 0 boundary migrate as a result of Kirkendall effect
- Type 0 boundary becomes diffuse
- Kirkendall markers move along curved path and marker plane bends around precipitates
- Diffusion path differs significantly from 1D calcul.

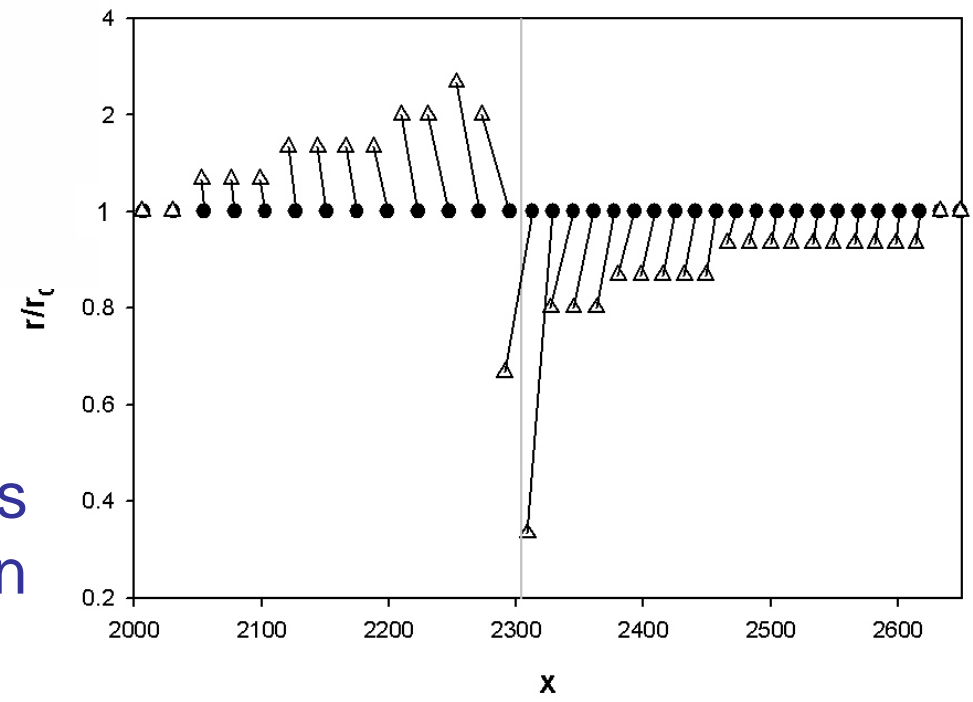


## Diffusion path: comparison with 1D simulation

*Wu et. al. Acta mater. 2001;49:3401*  
*Wu et. al. Acta mater, 2004; 52:1917*

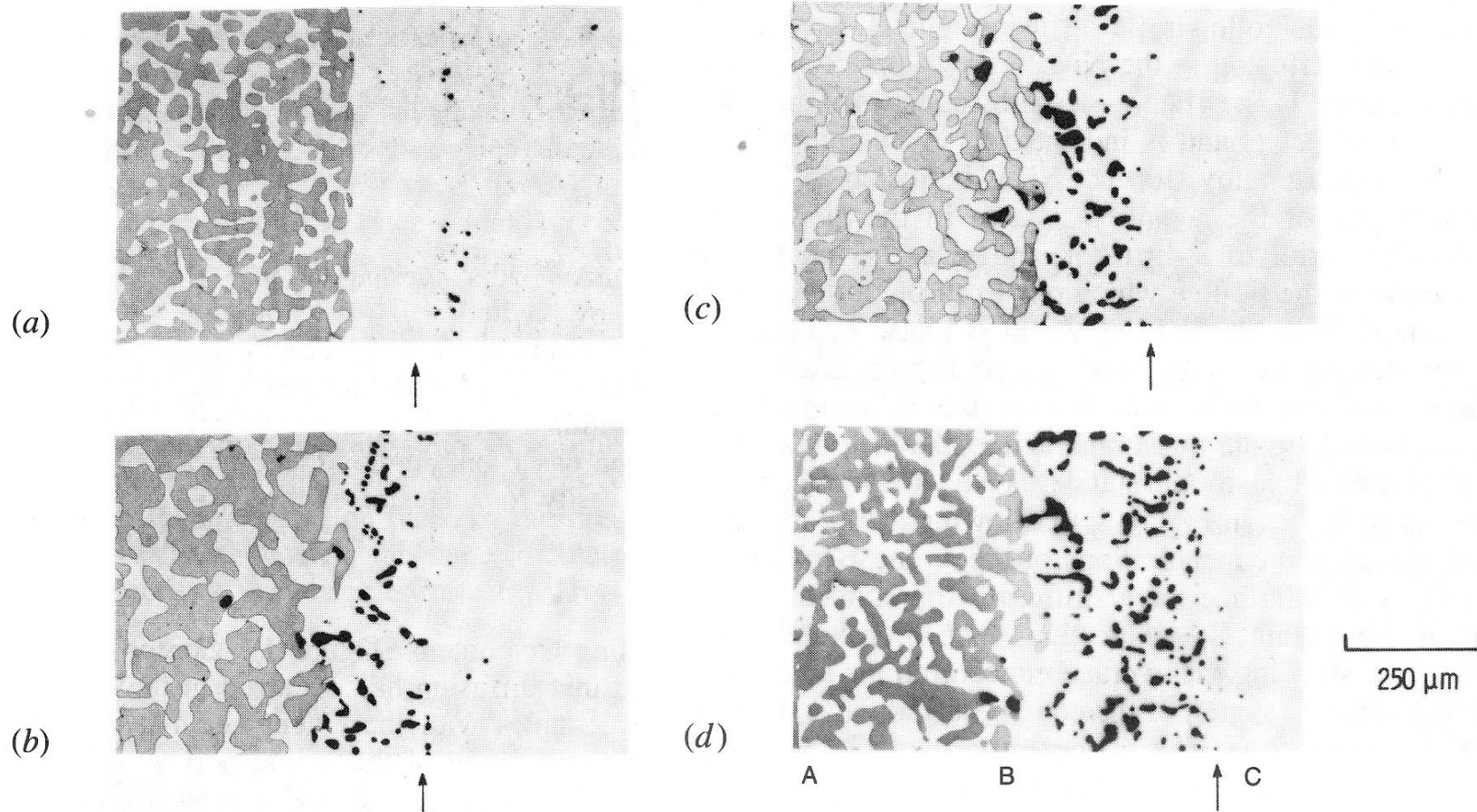


- 1D fixed boundary diffusion simulation
- ▲ 2D phase field simulation left half  $\tau=1600.0$
- △ 2D phase field simulation right half  $\tau=1600.0$
- major eigenvector direction at left half, 2D phase field
- major eigenvector direction at right half, 2D phase field
- major eigenvector direction at left half, 1D diffusion simulation
- - - major eigenvector direction at right half, 1D diffusion simulation



Size and position changes during interdiffusion

# Real Alloy System: Ni-Al-Cr

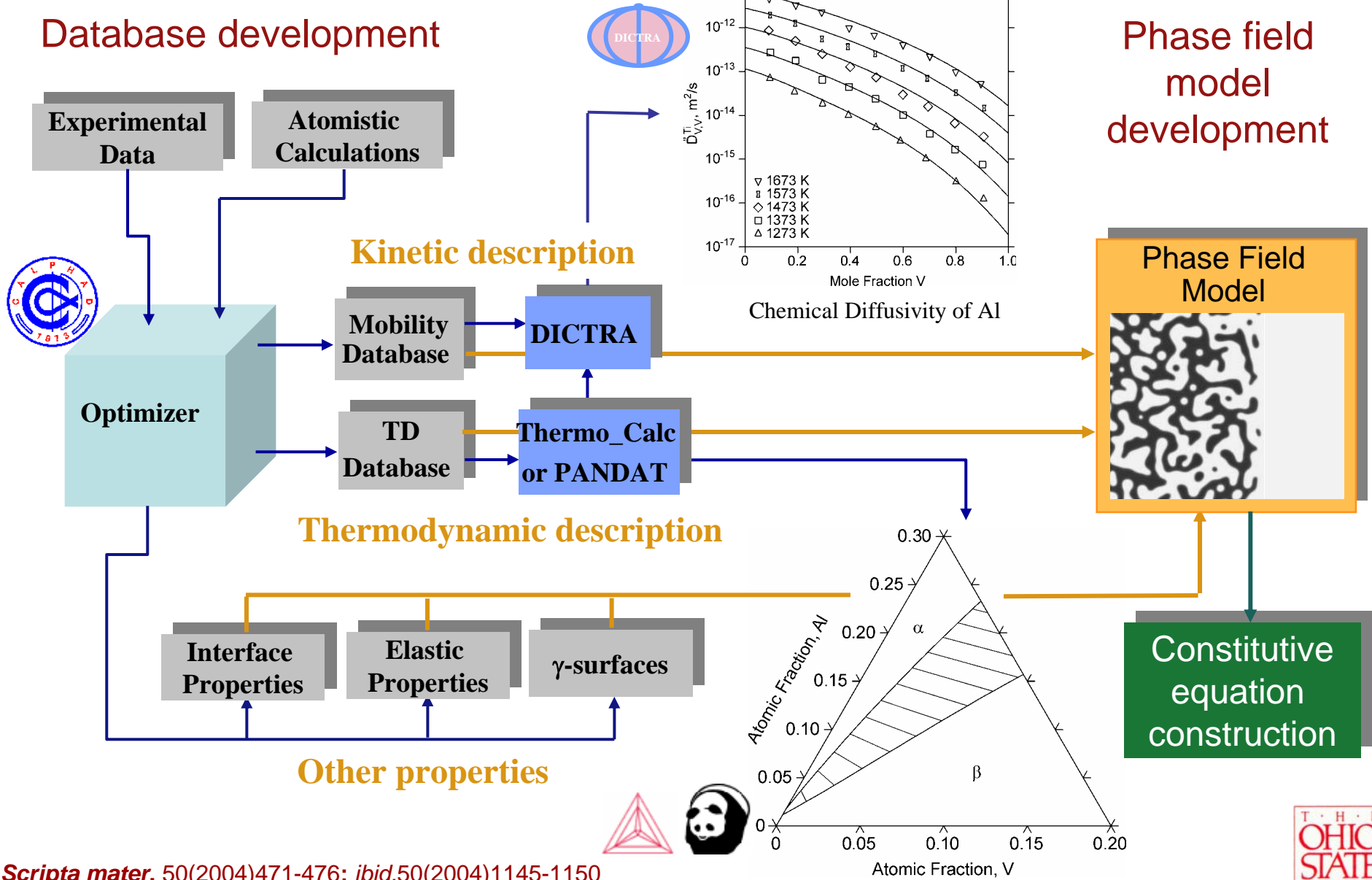


*Exp. Observation by Nesbitt  
and Heckel in Met Trans. A  
(1986)18A: 2087-2094*

Fig. 1—Microstructures of four  $\gamma/\gamma + \beta$ , Ni-Cr-Al diffusion couples after 100 h at 1200 °C. Arrows indicate original couple interface. Dark phase is  $\beta$ . Kirkendall porosity (black) is located in the diffusion zone (see Ref. 7). (a) Couple Ni-12.7Cr-24.0Al/Ni-45.5Cr,  $\beta$  recession = 120  $\mu\text{m}$ . (b) Couple Ni-12.7Cr-24.0Al/Ni-35.2Cr,  $\beta$  recession = 140  $\mu\text{m}$ . (c) Couple Ni-12.7Cr-24.0Al/Ni-25.0Cr,  $\beta$  recession = 205  $\mu\text{m}$ . (d) Couple Ni-12.7Cr-24.0Al/Ni,  $\beta$  recession = 320  $\mu\text{m}$ .

# Linking to Thermo. and Kinetic Databases and Atomistic Calculations

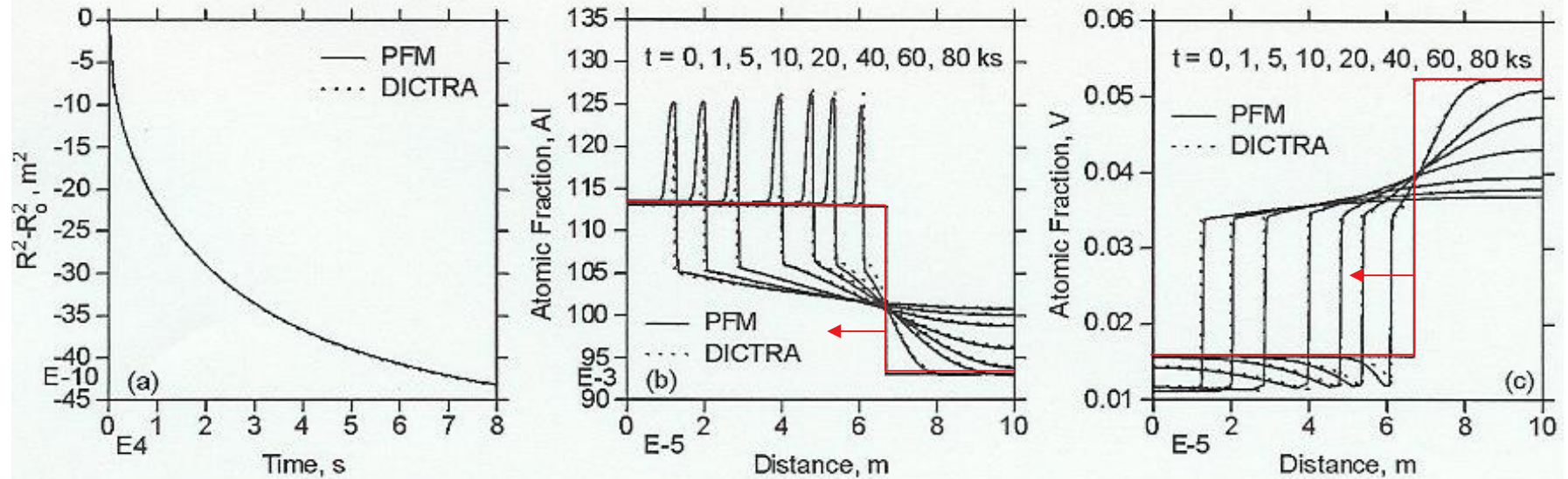
## Database development



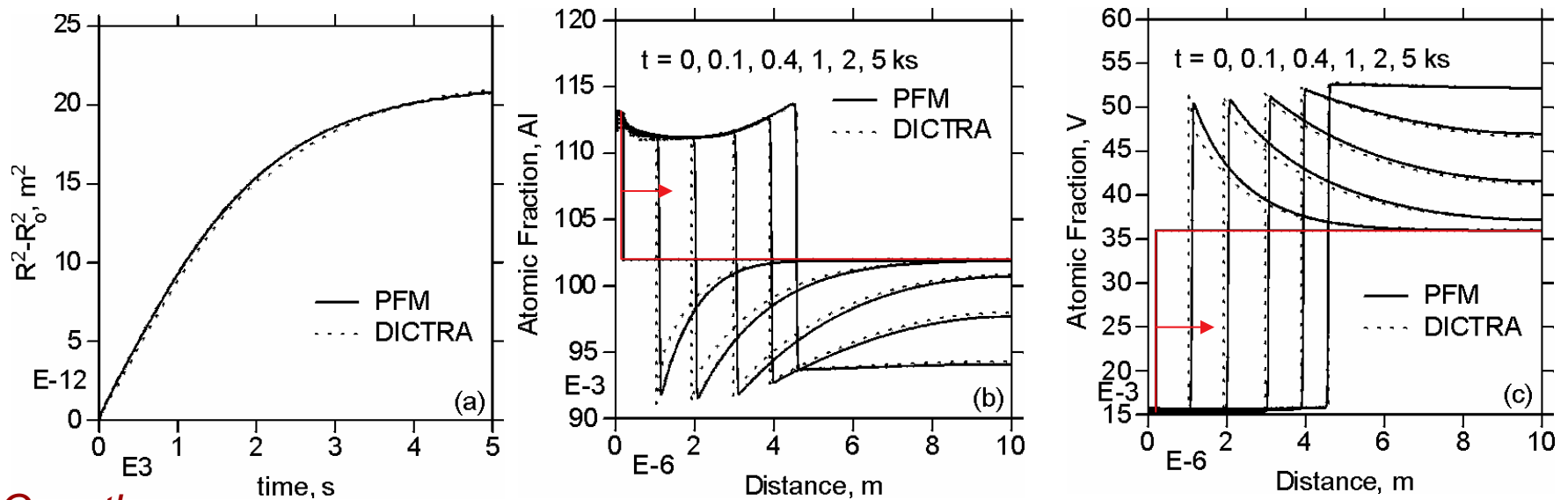
Scripta mater. 50(2004)471-476; ibid,50(2004)1145-1150

# Quantitative comparison with DICTRA

Q. Chen et. al. *Scripta mater.* 50 (2004)471-476

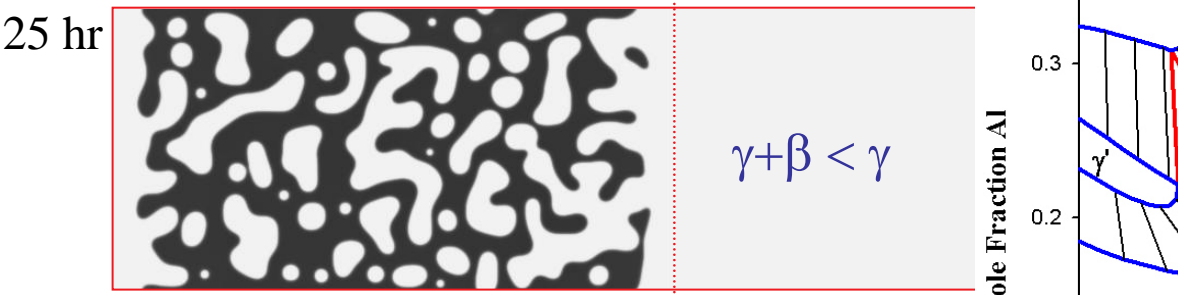
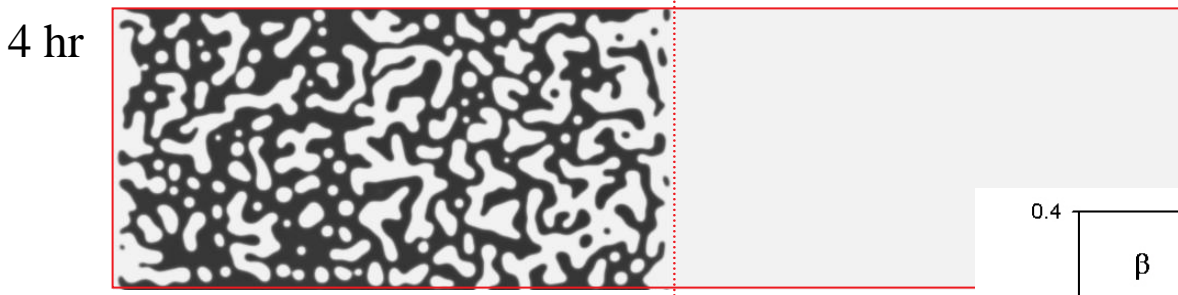
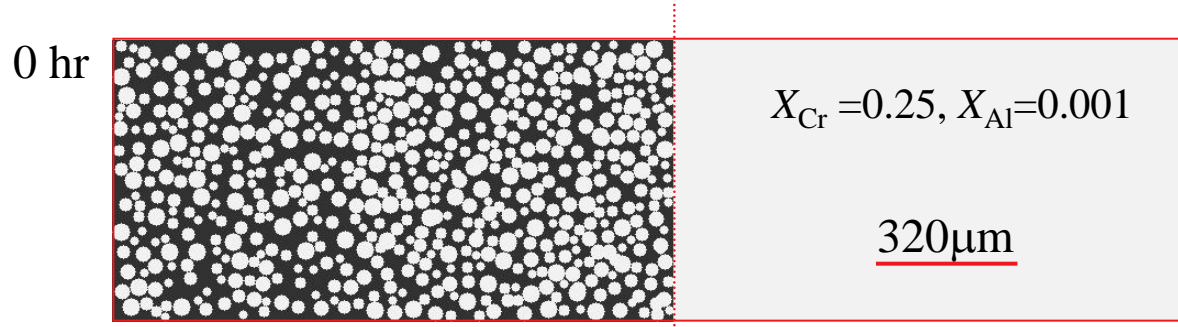


## Dissolution

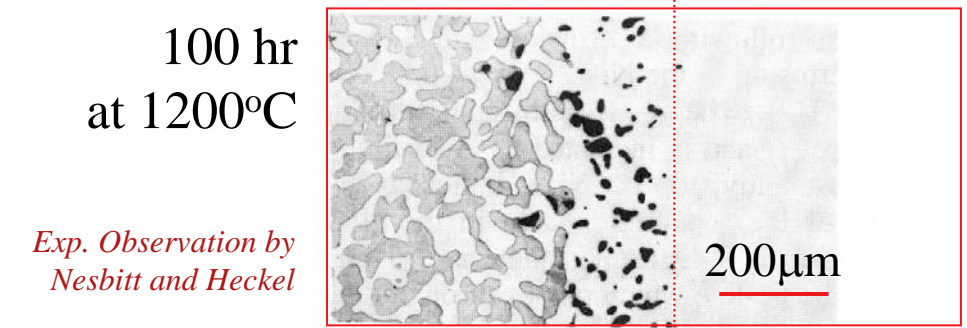


## Growth

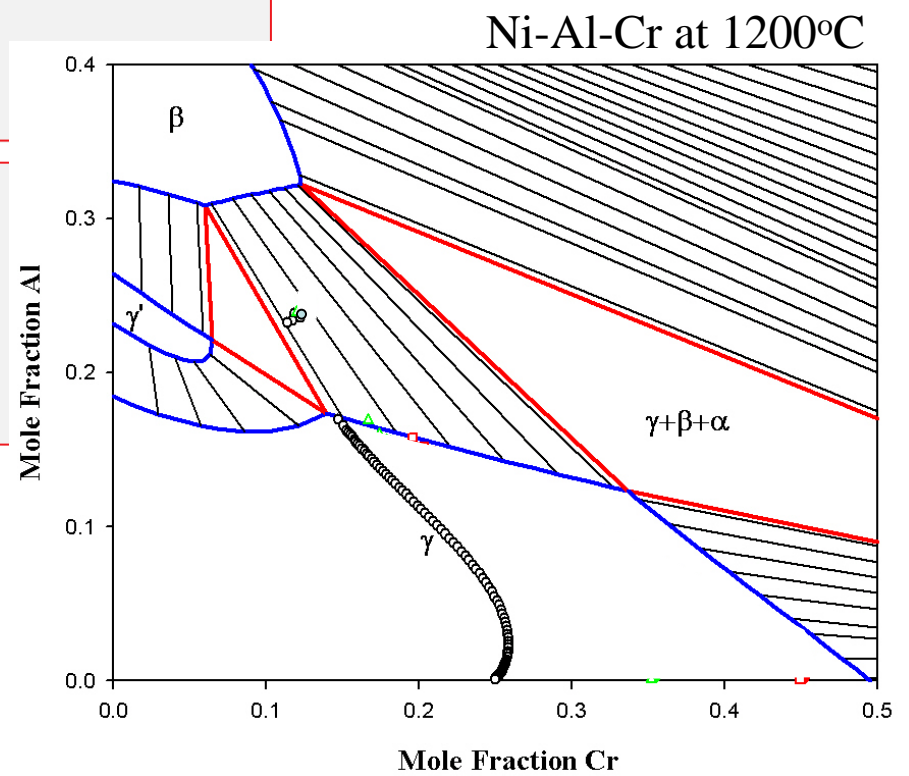
# Interdiffusion Microstructure and Diffusion Path



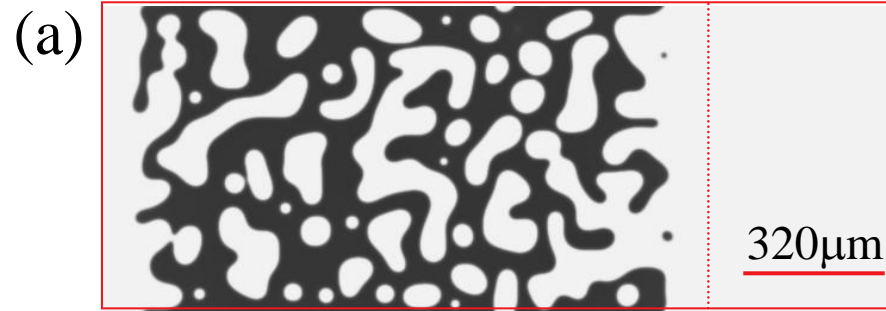
- Free energy data from Huang and Chang
- Mobilities in  $\gamma$  from A.Engström and J.Ågren
- Diffusivities in  $\beta$  from Hopfe, Son, Morral and Roming



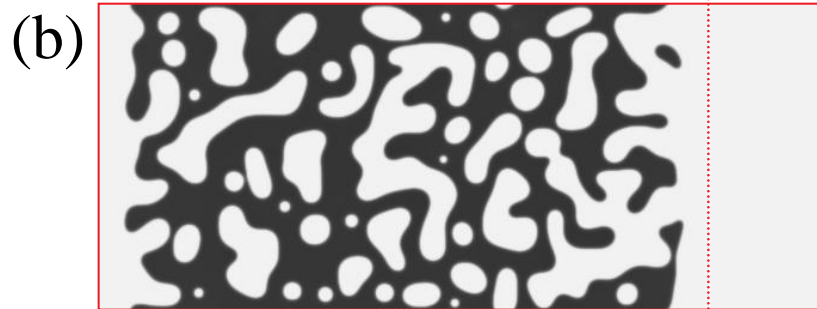
*Exp. Observation by Nesbitt and Heckel*



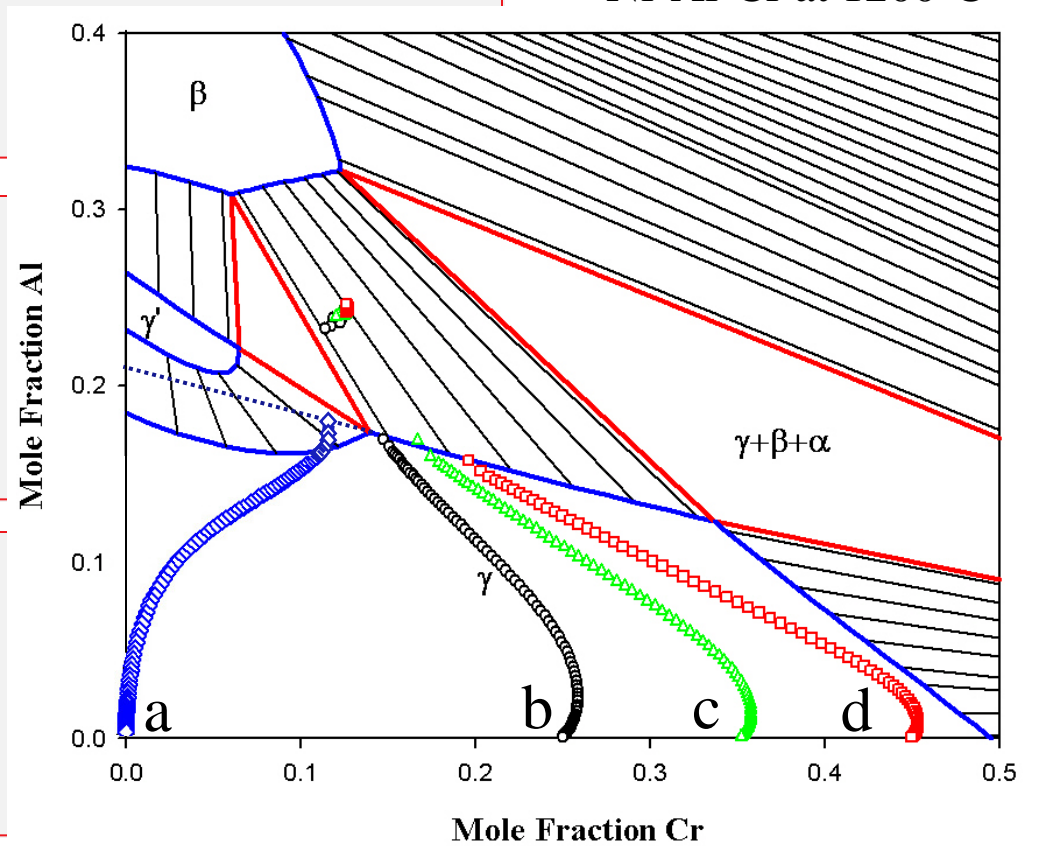
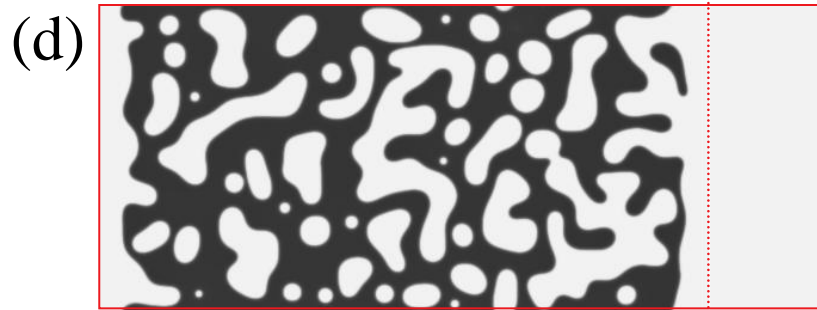
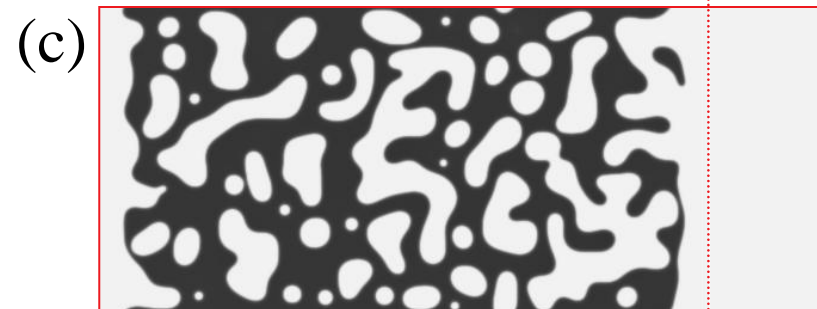
# Effect of Cr content on interface migration $\gamma+\beta < \gamma$



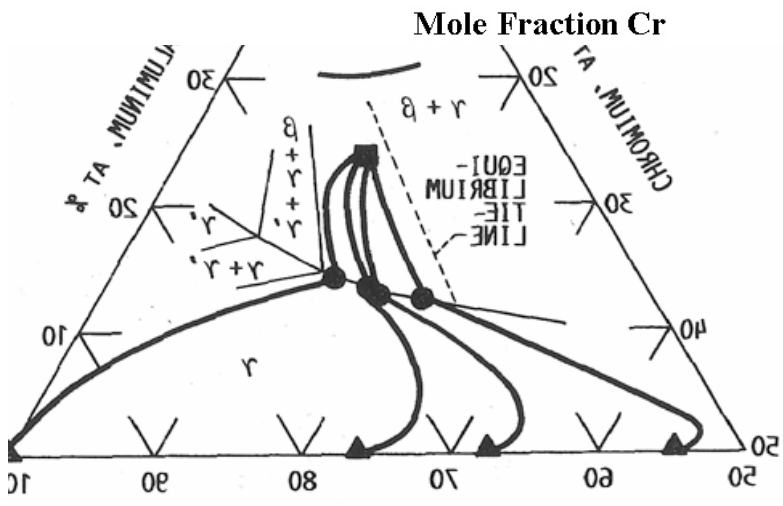
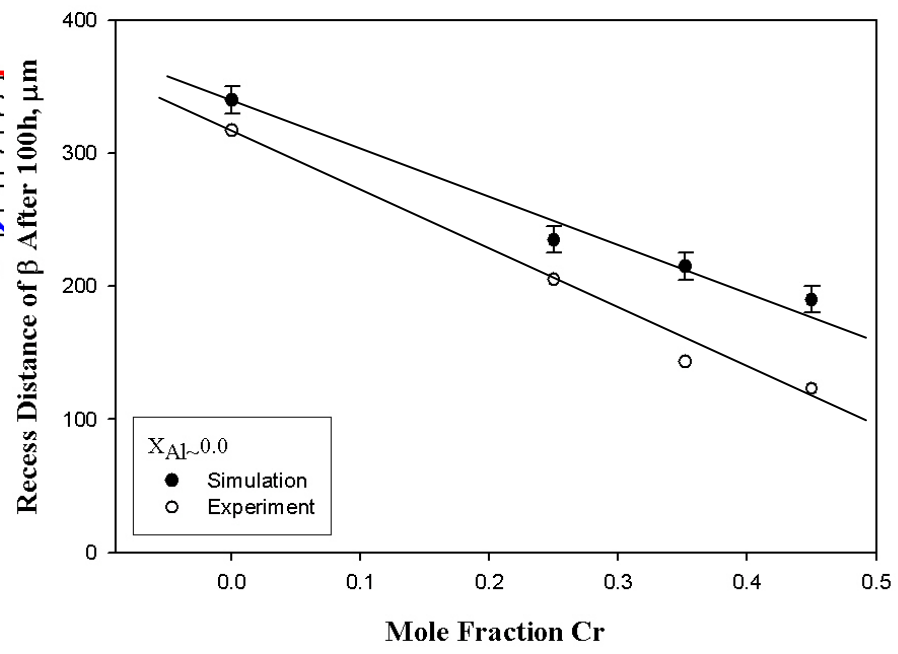
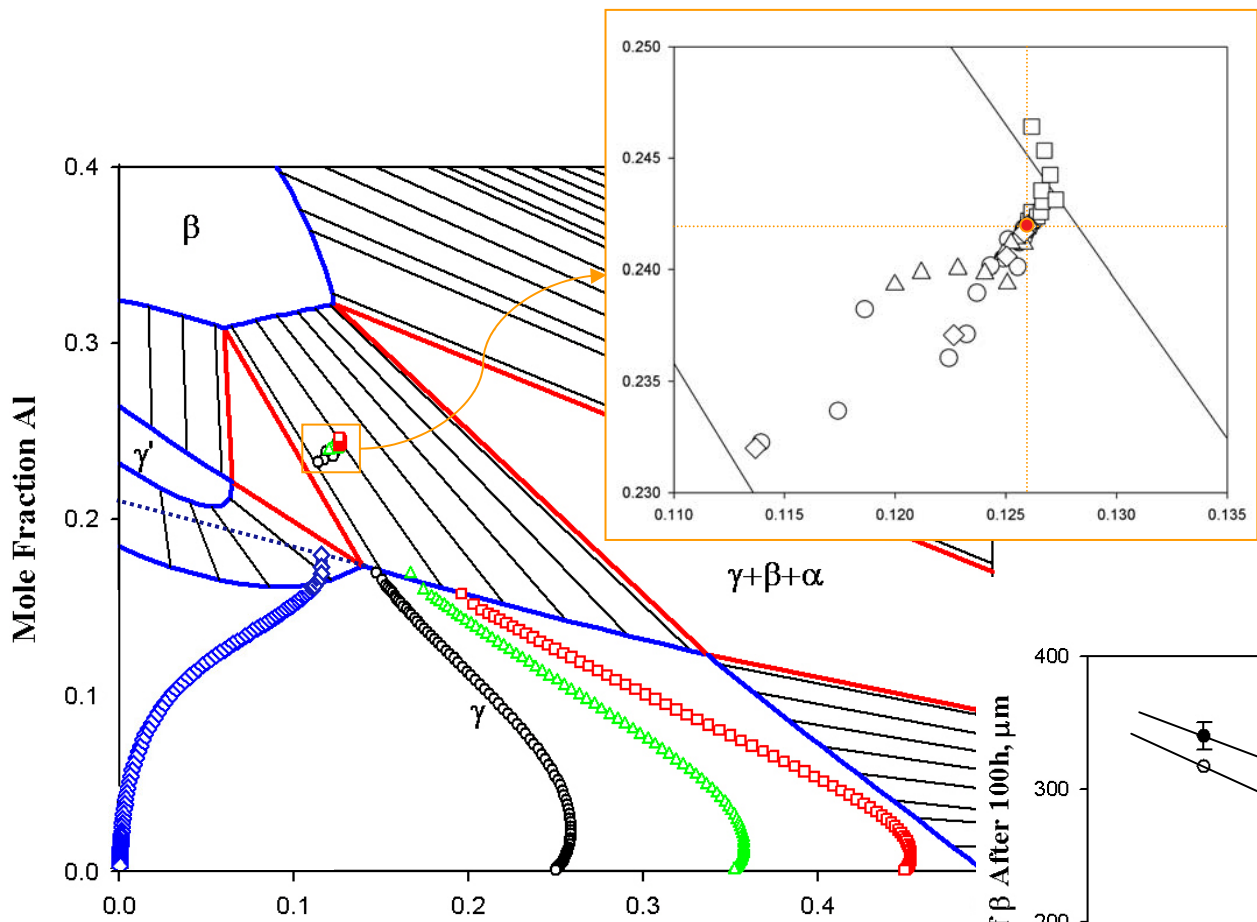
Annealing time:  
25 hours



Ni-Al-Cr at 1200°C



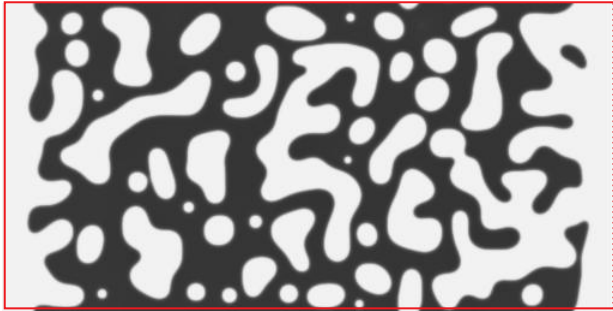
Diffusion path and recess rate - comparison with experiment



*Exp. measurement by Nesbitt and Heckel*

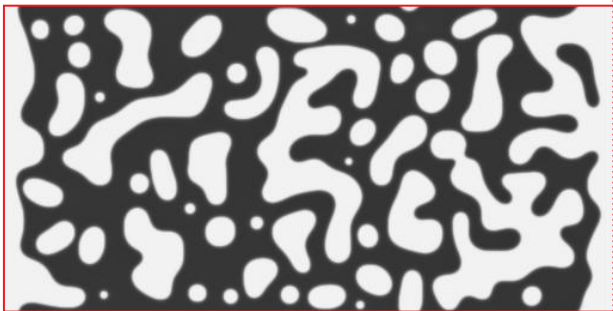


(a)

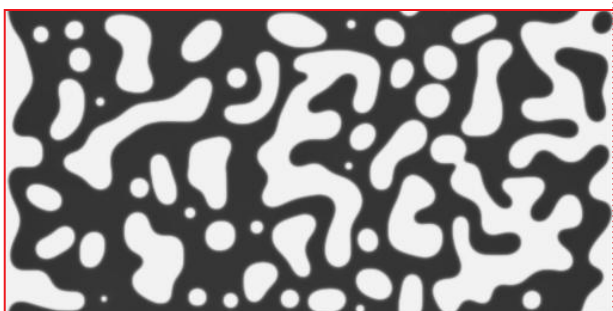


320μm

(b)

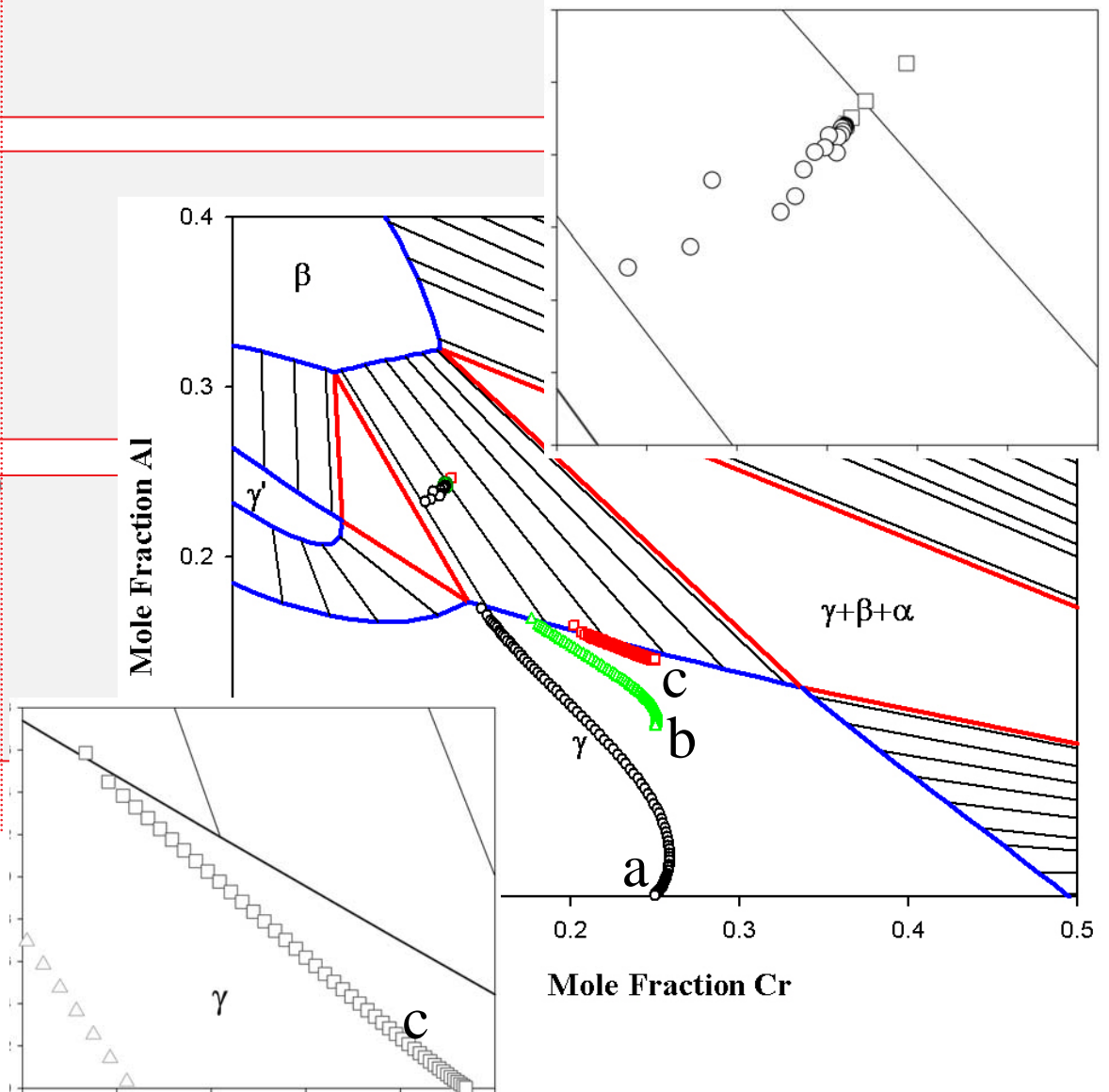


(c)



Annealing time:  
25 hours

Effect of Al content on  
interface migration  $\gamma+\beta < \gamma$



# Effect of Al content on interface migration

(a)

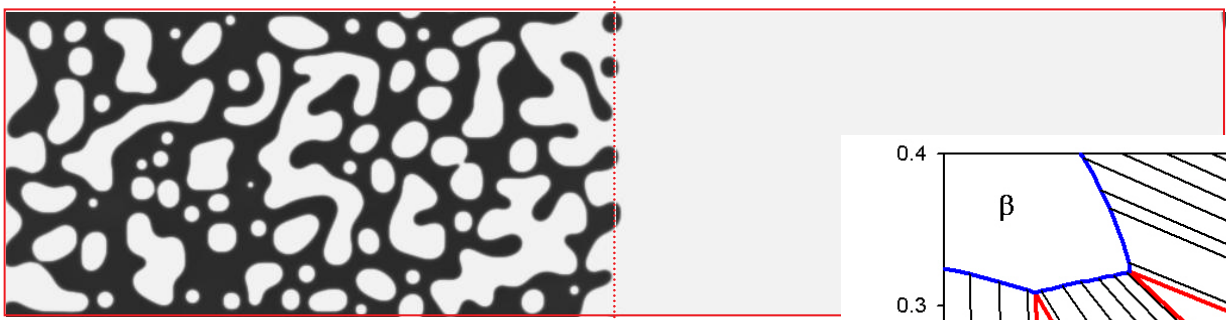


320μm

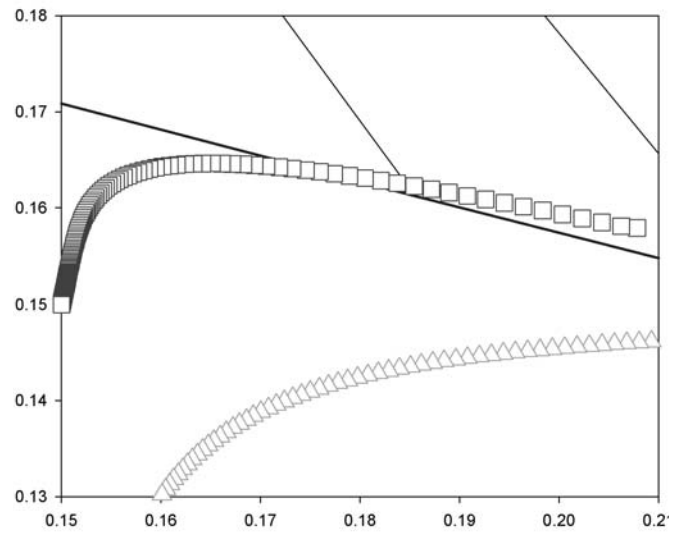
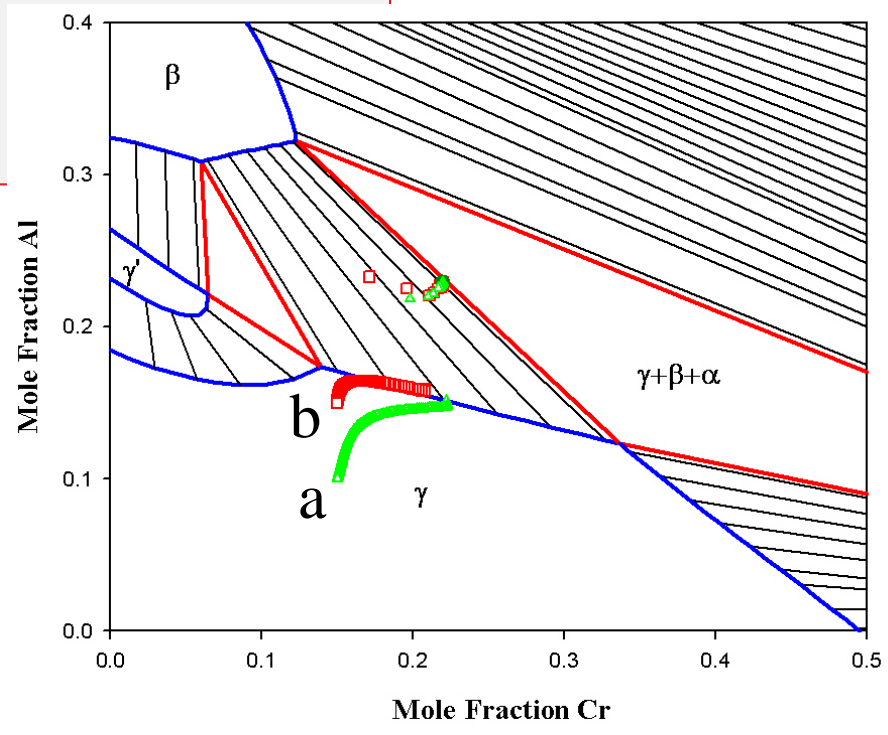
Annealing time:  
25 hours

$$\gamma + \beta < \gamma$$

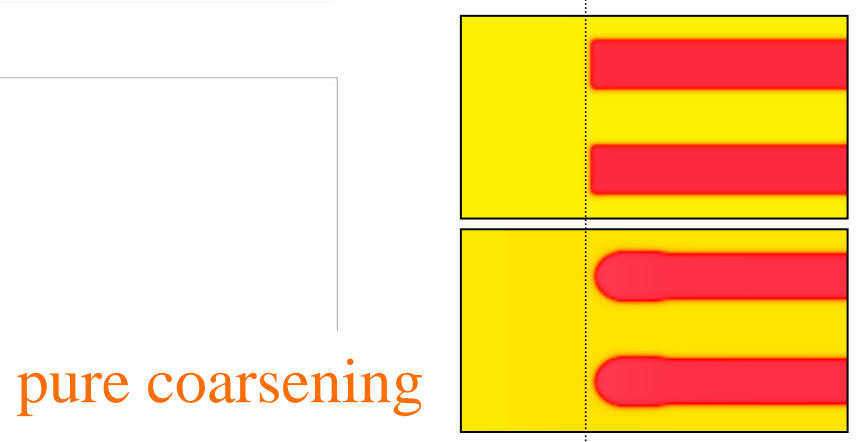
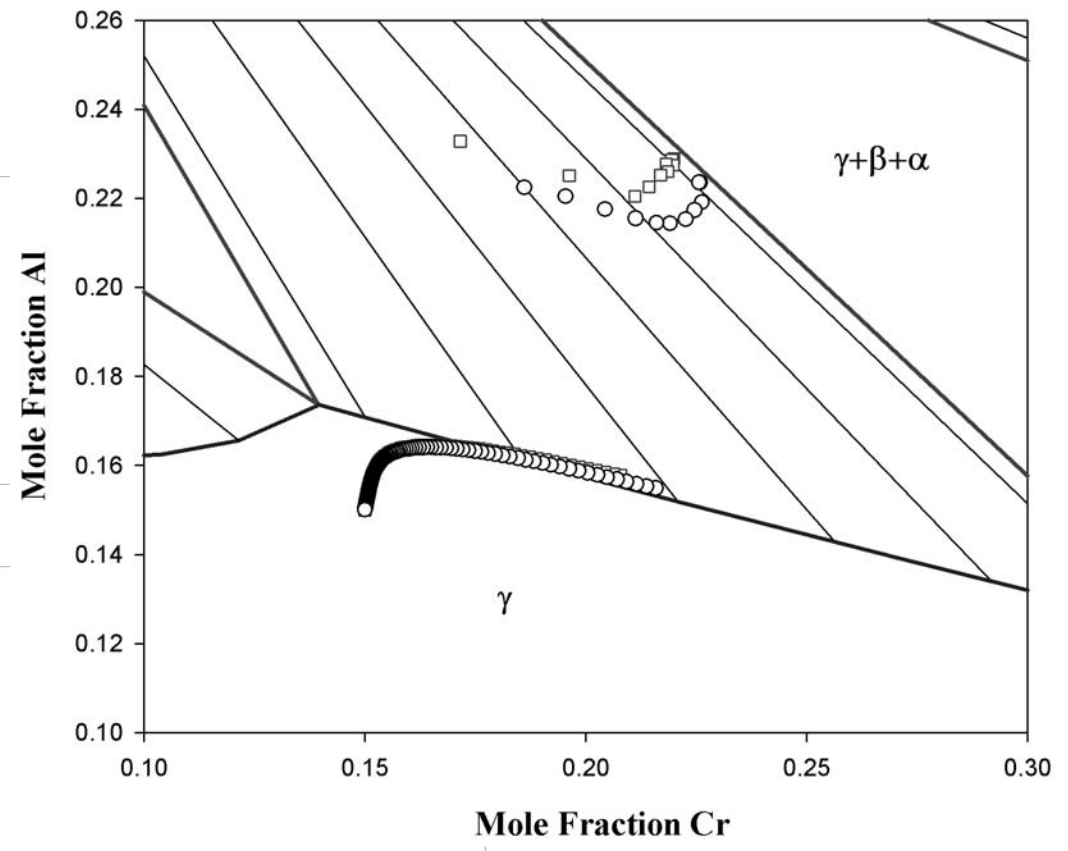
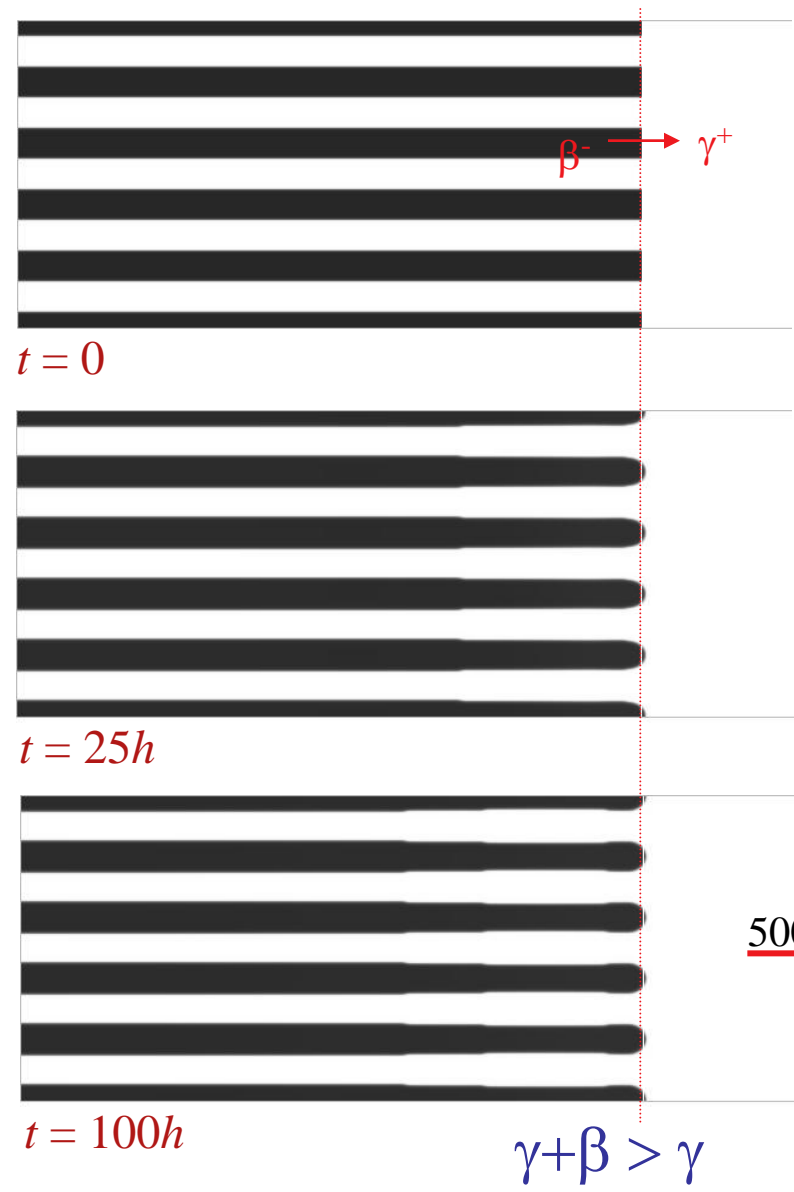
(b)



$$\gamma + \beta > \gamma$$

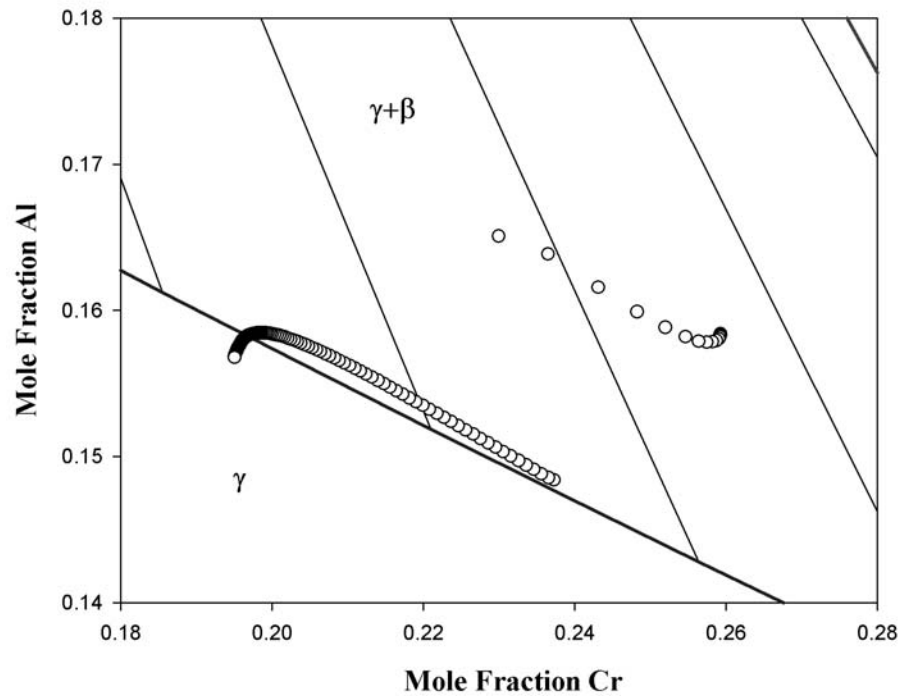


# Shape of the Diffusion Path

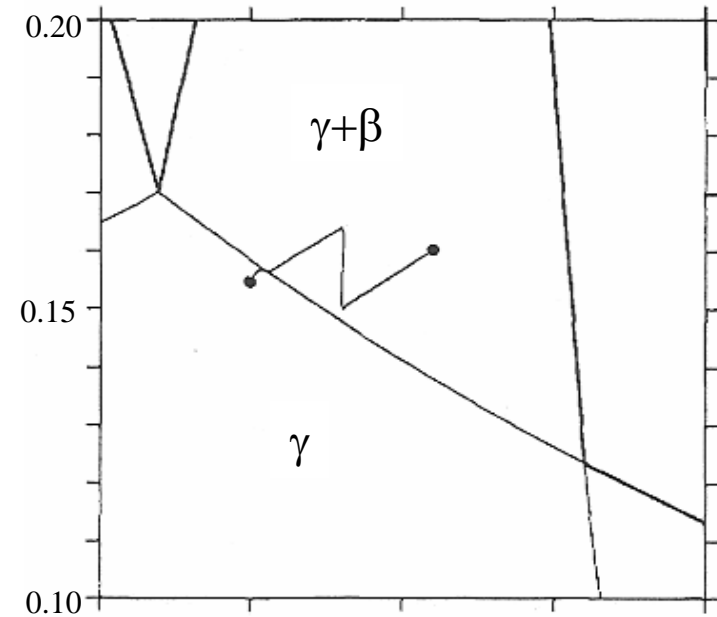


# Shape of Diffusion Path - Comparison with DICTRA

$$\gamma + \beta < \gamma$$



$$\gamma + \beta > \gamma$$



A. Engström, J. E. Morral and J. Ågren  
*Acta mater.* 1997

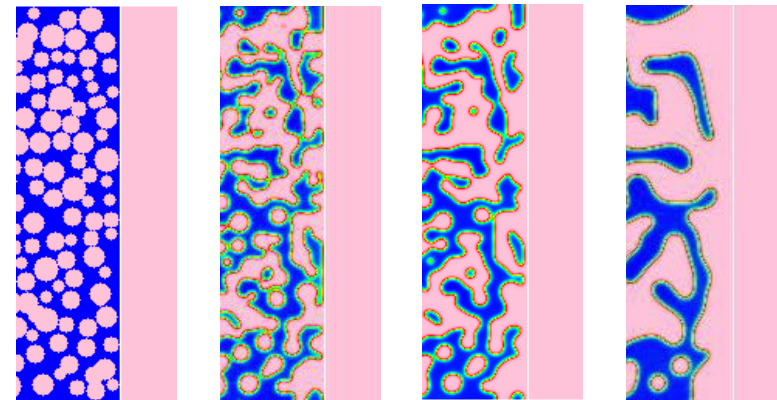
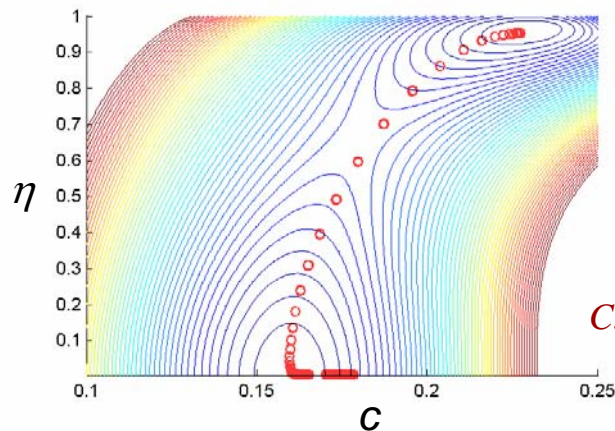
Growth vs. Nucleation

# Summary – Remaining Challenges

---

- Incorporation of nucleation
- Breaking the intrinsic length scale limit of quantitative phase field modeling

- effect of surface energy, e.g., coarsening and coalescence



*C. Shen et al., Scripta mater. (2004) 50:1023-1028; ibid, 1029-1034.*

- Quantitative comparison with experiment
  - accuracy of thermodynamic and mobility databases
  - accurate determination of average composition of multiphase microstructure in both simulation and experiment
  - Accurate determination of boundary position